SUNTEXT REVIEWS

SunText Review of Medical & Clinical Research
ISSN: 2766-4813

Open Access
Research Article
Volume 2:2

The Application of Magnetic Resonance Spectroscopy in Solid Tumors of Parenchymatous Organs: Literature Review and Own Experience

Iosefi DY[1], Vinidchenko MA[2,*], Demchenko NS[3]

Rostov Scientific Research, Cancer Institute, Ministry of Health of Russia, Rostov-on-Don, Russia

[*]**Corresponding author:** Vinidchenko MA, Rostov Scientific Research, Cancer Institute, Ministry of Health of Russia, Rostov-on-Don, Russia; E-mail: vinidchenko@mail.ru

Received date: 19 April 2021; **Accepted date:** 30 April 2021; **Published date:** 02 May 2021

Citation: Iosefi DY, Vinidchenko MA, Demchenko NS (2021). The Application of Magnetic Resonance Spectroscopy in Solid Tumors of Parenchymatous Organs: Literature Review and Own Experience. SunText Rev Med Clin Res 2(2): 131.

DOI: https://doi.org/10.51737/2766-4813.2021.031

Abstract

The article provides an analysis of publications devoted to proton MR spectroscopy in vivo with an emphasis on its application in pancreatic and prostate cancer in the context of solving complex differential diagnostic problems of modern oncology. Clinical cases from our practice of using single-voxel spectroscopy in prostate and pancreatic cancer are presented, and the diagnostic significance of the inclusion of MR- spectroscopy in the scanning protocol in comparison with native scanning protocols.

Keywords: Magnetic resonance spectroscopy; Pancreatic cancer; Prostate cancer; Lactate; Lipids; Citrate

Introduction

Relevance and current state of the problem. Proton magnetic resonance spectroscopy (MRS) for hydrogen was theoretically developed in 1951. MRC of intact biological tissues was first reported by two groups: R. B. Moon and J. H. Richards, who used P-31 MRC to study intact red blood cells in 1973. using P-31 MRC to study the excised leg muscle of a rat in 1974 [1, 2]. The first MR spectrum of the human brain in vivo was published in 1985 by P. A. However, the gradual expansion of the application and the accumulation of clinical, biochemical, and tomographic material intensifies the use of this technique in the pathology of the prostate, pancreas, liver, and other parenchymal organs. Unfortunately, the active use of MRS in vivo in the abdominal cavity and pelvis is limited by spectral resolution, signal-to-noise ratio (SNR), and motion. MRC allows noninvasively obtaining information about the chemical composition of the tissue and provides an additional characteristic of the isolated volume (voxel) of the lesion based on the analysis of the concentration of cellular metabolites. The maximum spatial resolution of the method is approximately 0.5 cm3. The MRS registers signals from chemicals in the tissues or metabolites. The peaks of the metabolites are identified primarily by their frequencies (their position in the spectrum) and are expressed as a frequency shift in parts per million (ppm) relative to the standard. The most common nuclei used for in vivo MRC are hydrogen protons (1H), sodium atom nuclei (23Na), and phosphorus atom nuclei (31P). The advantages of 1H spectroscopy are that it is easier to perform, more widely available, and provides a much higher signal-to-noise ratio (SNR) than 23Na and 31P. In NMR spectroscopy, the frequency of the location of a metabolite or chemical compound depends on the configuration of protons within the chemical. There is a lot of water in biological tissues, and its frequency location is used as the standard for 1H MRC in vivo, meaning that all other chemicals are identified by comparing their frequency location (frequency shift) with that of water. 1H MRC is usually included in standard MR imaging protocols to obtain functional information and can be performed in 5-15 minutes. The most studied metabolites, taking into account their peaks in proton spectroscopy, are choline with a peak of 3.2 ppm; acetylaspartate-2 ppm; myoinositol-3.56 ppm; fat compounds-1-1. 2 ppm; glutamate – 2.2-2.5 ppm; creatinine-3-3. 9 ppm [3] (Figure 1).

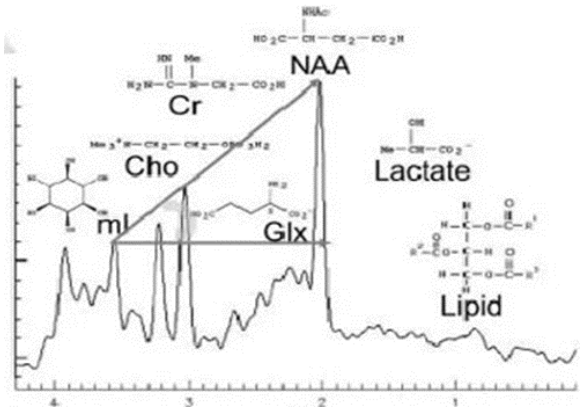

Figure 1: *Typical position of the peaks of various compounds in the MRS of normal brain tissue.*

The main research and developments of MRS are carried out in the field of oncology. Free and commercial software is available with various algorithms for post-processing MPS data. Post-processing includes motion correction (correction for frequency and phase shifts), automatic water suppression, and low-frequency filtering of the residual water signal, Fourier transformation, and Lorentz and Gaussian transformations. These actions can be fully automated. Observations reveal an altered ratio of choline-creatinine, N-acetylaspartate, and creatine metabolism in most malignancies. Some cancers are accompanied by an increase in the peak of lactate in proton MRS. The graphs of metabolites of normal liver parenchyma and fatty dystrophy (steatohepatosis) are clearly (Figure 2).

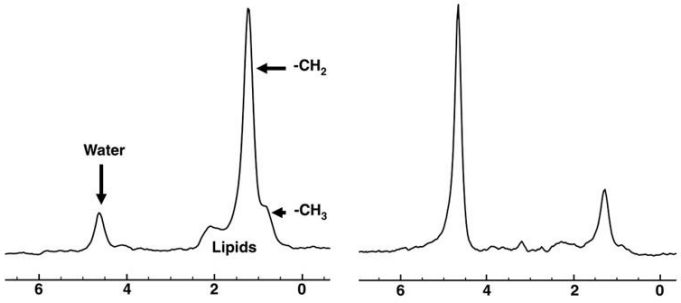

Figure 2: *Comparison of water and lipid peaks: a-with fatty liver dystrophy, b-normal.*

The use of MRS is based on significant differences in the ratio of metabolite peaks in tumor tissues and in radiation necrosis, which were established in most studies devoted to this problem [4, 5]. For example, the spectral pattern of radiation necrosis includes a decrease in the concentration of choline (Cho), creatine and N-acetylaspartate (NAA), as well as the presence of lactate peaks (Lac), lipid complex and other metabolites [6]. Lactate (Lac) is the end product of anaerobic glycolysis, a marker of hypoxia. In healthy volunteers, the lactate concentration is at the level of the sensitivity limit of the method, that is, it is usually not detected on the spectra. Increases with ischemia, tumors. The double peak of lactate is at 1.33 ppm, and at TE 135 ms it is inverted (is in antiphase), at TE 30 ms it is directed upwards (is in phase). The Warburg effect is known - the tendency of cancer cells to produce energy mainly through very active glycolysis followed by the formation of lactic acid [7,8]. These changes are one of the characteristic effects of cancer-causing mutations and metabolic markers of pathological tissue. The potential benefits of lactate-mediated acidosis for cancer cells are numerous. The acid-modified invasion hypothesis suggests that H+ ions secreted by cancer cells diffuse into the environment and alter the tumor-stroma interface, providing increased invasiveness [9]. Moreover, lactate obtained from the tumor contributes to the polarization of tissue macrophages [10]. The Warburg effect is thought to be an early event in oncogenesis that is a direct consequence of an initial oncogenic mutation, such as the KRAS mutation in pancreatic cancer [11]. Lipids (lip) – an indicator of necrosis and destruction of myelin sheaths. Usually not detected in healthy volunteers, they increase with tumors, necrosis, abscesses and demyelination. Peaks at 0.8 and 1.3 ppm. The signal from lipids is best detected at low TE values (less than 35 ms) and decreases at higher TE values. Since Lac and Lip resonate at the same frequency of 1.3 ppm, in the case of the presence of both metabolites in the study area, their peaks may be indistinguishable or overlap and interfere. To highlight the Lac peak, the following points are considered important: Lac has a double peak; At TE of the order of 135 ms, the Lac peak is inverted; when using high TE values (270 ms), the Lip signal is suppressed and only the Lac signal remains. The peak of lipids reflects tissue necrosis, and the increase in lactate is caused by concomitant ischemia. With a variable diagnostic threshold of digital values, an increase in the Cho/Cr and Cho/NAA ratios in the tumor tissue was found, as opposed to their decrease in the post-radiation lesion. An interesting fact is that a lower NAA/Cr ratio is observed in the tumor tissue (in the foci of glioblastoma necrosis) than in the tissue with radiation necrosis. A review of published studies shows that MRS is a useful method for the differential diagnosis of continued tumor growth and radiation necrosis, although not all studies indicate significant differences in their spectral characteristics [4]. In a viral disease, Cho and Ins always increase, whereas a decrease in NAA mainly reflects a deeply altered clinical condition and cytolysis. In bacterial abscesses, the content of many amino acids, lipids, and Lac may be increased [12]. A model is known in which the MRS profile of myo-inositol (Ins), glutathione (GSH), and total choline (GPC+PCho) will detect aseptic inflammation even in the absence of other significant changes on MRI, and an increase or decrease in the concentration

of markers over time will differentiate the prognosis of the process - whether the inflammation will be persistent or attenuated. Practitioners often have to rely only on subjective indicators to diagnose the therapeutic pathomorphosis of the tumor and to assess how the patient responds to treatment [13]. Even the introduction of scales similar to the TRG (tumor regression grade) does not eliminate the subjective component. Thus, there is a need to objectify the in vivo detection of inflammation, including infection, by non-invasive methods. One of the remaining problems of using the method is the variety of estimates of the MRC data with the calculation of different ratios (taking into account the small value of the signal against the background of the water peak). Moreover we still face the insufficient consensus in choosing the most diagnostically accurate path of analysis, as well as the deficiency of histopathological verification of the results (due to the problem of combining the spectroscopic voxel with the biopsy point in heterogeneous processes). The limitations of the method are also associated with predictable and probably irremediable errors in the combination of tumor tissue with post-radiation changes [14]. In a study,the Lip-Lac/Cho and Lip-Lac/nCr ratios distinguish a pure tumor from a pure necrosis [15]. No values suggested that mixed samples could be statistically significantly distinguished from either pure tumor or pure necrosis. These studies show the importance of choosing the location of the spectroscopic voxel in a homogeneous area of the histopathological process. It is also known that it is possible to bring non-invasive verification techniques to a new level. Using state of the art technology in the study, the ratios of Cho/Cr (choline-containing compounds / creatine-phosphocreatine complex), Cho/NAA (N-acetyl aspartate) and NAA/Cr were evaluated by spectral maps in the tumor nucleus and peritumoral edema [16]. Differences in the ratio of metabolites between low-grade anaplasia gliomas (LGG), malignant gliomas (HGG), and metastases were statistically analysed. The lipid / lactate content was also analyzed. There were significant differences in tumor and peritumoral Cho/Cr, Cho/NAA, and NAA/Cr ratios between LGG, HGG, and metastases. The content of lipids and lactate was useful for distinguishing between gliomas and metastases. The results of this study demonstrate that MRS can differentiate between LGG, HGG, and metastases. So the diagnosis can be reliably established and verified even in patients who cannot undergo a biopsy. With regard to extracerebral diseases, spectroscopy has not become a mainstream technique. In the literature and studies on diffuse liver diseases, phosphorus spectroscopy is considered promising [17-20]. However, there are not enough publications on the informative value of the MRS technique and the prospects for its application in relation to focal liver pathology, which is due to the difficulties of post-processing, positioning the patient with the placement of the zone of the most interesting changes in the magnet isocenter for spectroscopy, equipment requirements, and comparison with morphological data. The increase in the content of phosphomonoester (PME) in cancer occurs due to the proliferative activity and synthesis of phospholipid membranes. Similar changes are detected in cirrhosis, but they are more pronounced in tumors. An increase in the PME content is determined not only directly in the tumor node, but also in almost the entire liver tissue. Probably, this fact can be explained by a complex restructuring of the processes of energy metabolism in the body of an oncological patient with an increase in glycolysis and inhibition of plastic metabolism. One of the main manifestations of this rearrangement is the proteolisis and the acceleration of glucose consumption, in response to which the body reacts with an increase in gluconeogenesis, which is accompanied by an increase in the content of the corresponding intermediates, such as glucose-6-phosphate, etc., which are involved in the creation of the PME peak on the phosphoric MR spectrum. Several in vivo MRC studies have reported an increase in choline levels in tumors, such as hepatocellular carcinoma, and a decrease in the lipid-to-choline ratio after transarterial embolization performed for hepatocellular carcinoma [23,24]. The PME/PDE ratio in the liver in vivo decreased in patients with hepatitis C who responded to antiviral treatment, and remained the same or increased in patients without a virological response. These results suggest that PM and PDF may be used as biomarkers in a non-invasive treatment response test.

A typical case of proton MRS from the archive of the department of MRI of the national research center of oncology

In the study of the MRC of the verified metastasis of neuroendocrine pancreatic cancer to the liver, the picture of the peak from fat, lactate was obtained on the inverted spectra (Figure 3,4).

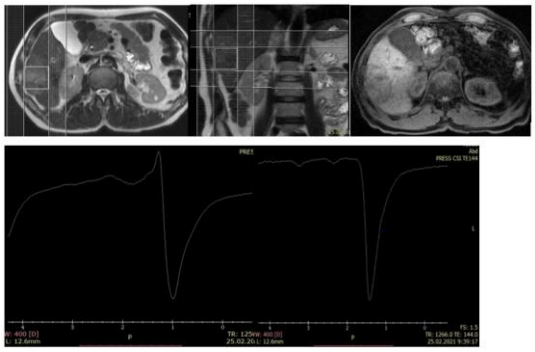

Figure 3: *Inverted spectra with values of TE=35 ms and TE=144 ms from the metastatic focus in the liver, localization of the bill and saturation areas. In the upper row of the image in the T2-axial sequence, T2-coronal sequence and axial LAVA-sequence of metastasis of neuroendocrine pancreatic cancer to the liver.*

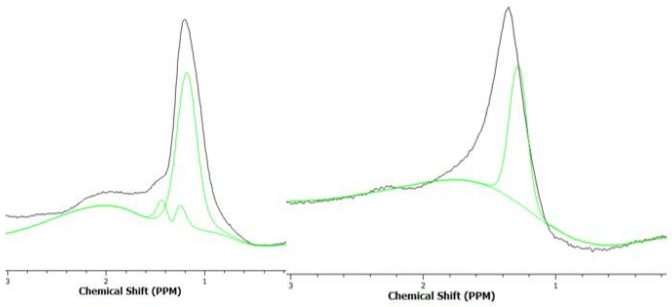

Figure 4: *The spectra analyzed in Tarquin with values of TE=35 ms and TE=144 ms of metastasis of neuroendocrine pancreatic cancer to the liver, the green lines reflect the frequency analysis of the signals of the lactate-lipid complex, the black lines represent the total signal.*

In the study of the prostate, proton and phosphor spectroscopy are mainly used. The main metabolite of the normal prostate is citrate, which is part of the secret of the gland. The maximum amount of citrate is contained in its peripheral zone-30.9±8.5 mmol/g. The total citrate content in a normal prostate is 4-6 micromol/g. In the tumor cell, the citrate content decreases, which is explained by a distortion of the metabolism in the tumor cell, namely, the synthesis of citrate is replaced by its oxidation. According to various authors, the citrate concentration in prostate cancer ranges from 1-2 to 3.74 mmol / g, whereas in the normal prostate, the total citrate content is 4-6 mmol/g. The content of creatine and creatine phosphate, which in a healthy cell are used in energy exchange, decreases in malignant processes. This is due to a decrease in the total level of ATP in the tumor cell. Also, in the tumor tissue in prostate cancer, as well as in hepatocellular carcinoma and metastases to the brain and liver, the content of substances involved in the synthesis of lipids, such as choline, inositol, and phospholipids, increases sharply. In tumor cells, the synthesis of proteins necessary for the construction of the cytoplasm is increased, so there is an increase in the content of many amino acids, including alanine and glutamate [25,26]. It is believed that the absence or sharp decrease in citrate content in prostate tissue is pathognomonic for adenocarcinoma, although the choline+creatine/citrate or citrate/choline+creatine ratio is much more often used for the diagnosis of prostate cancer. In prostate cancer, higher values of the choline+creatine/citrate ratio are detected than in the normal peripheral zone. An excess of this ratio of more than 0.75 or a twofold decrease in the citrate peak compared to the norm is characterized by high predictive value (75%) and high specificity (84%) for prostate cancer. The sensitivity and predictive value of a negative result are 71% and 81%, respectively. The values of the citrate/choline+creatine ratio in the tumor tissue (0.67 ± 0.17) are correspondingly lower than in the healthy peripheral zone (1.46 ± 0.28). When using the surface coil, significant differences in the citrate/choline+creatine value were obtained between cancer (0.446 ± 0.063) and the healthy transient zone, although no significant differences were obtained between cancer and benign stromal gland hyperplasia. Combining multi-pixel spectroscopy with standard T2-weighted images can not only improve the detection of prostate cancer, but also obtain spatial information about the localization of cancer. The causes of low-intensity signals, in addition to cancer, can be post-biopsy hematomas, prostatitis, benign hyperplasia, and dysplasia. Therefore, some researchers suggest using the choline+creatine/citrate ratio for the differential diagnosis of low-intensity signals. They showed that by adding three-dimensional proton spectroscopy to MRI, it is possible to achieve a significant increase in accuracy (from 52 to 75%) and specificity (from 26 to 66%) in the detection of tumors in the area of post-biopsy haemorrhages. With the help of MRC, it is possible not only to detect prostate cancer and determine its localization, but also to predict the severity of histological changes according to Gleason. With a sharp increase in the choline peak spectrum, 7-8 points are predicted, and with a moderate increase - 4-5 points, the Gleason score. The experience of using prostate MRS, accumulated in the MRI department at the NMRC of Oncology, is mainly reduced to single-voxel MRS, while the voxel was located on the most highly rated DWI and T2 images in accordance with the PiRADS criteria. Patient B., 60 years old, went to the doctor due to symptoms of obstruction of the lower urinary tract. In the anamnesis - transrectal biopsy with G1 adenocarcinoma verification, Gleason index 6 a year before MRI, PSA-11.8 ng / ml in September 2019, did not receive special treatment before treatment. Peripheral zone: reduced, the lobes are asymmetric, with the presence of post-biopsy changes, the foci of the infiltrative lesion in both lobes at the median level, the largest lesion on the left peripheral zone at the median level (PZa-PZpl) according to PIRADS v2 was estimated as 5 points. An increase in choline and a decrease in citrate in the volume of the lesion were confirmed, the values of the choline+creatine/citrate ratio reached 0.83, which confirmed the presence of malignancy without repeated biopsy. In a study on a rat model of carrageenan-induced intestinal inflammation, the metabolites include creatine, phosphatil choline, the CH2HC group in the fat chain of alkyls, and the glycerol backbone of lipids [27]. The differences in the concentrations of these metabolites in each group gave us an idea of the biochemical changes that occur during inflammatory diseases of the large intestine, and create the diagnostic potential of 1H MRC as a tool for future studying inflammation in combination with biopsy, despite ex vivo, the materials are promising for transfer to the studied peritumoral inflammatory processes, but the technique requires calibration and refinement.

Materials and Methods

To study the diagnostic value of the developed model, the sensitivity, specificity, and overall accuracy of the abdominal MRI were calculated in patients with ductal pancreatic adenocarcinoma based on the signs of the presence of solid tumor tissue. The study included 20 study protocols of patients who went to the department to clarify the diagnosis at the initial detection of ductal pancreatic adenocarcinoma and 20 patients with chronic pancreatitis. The studies were performed on a GE Signa 1.5 THD tomograph on a surface 8-channel coil according to a protocol that included visualization in T2-VI, T2-fatsat, LAVA, T1-fatsat, Dual-echo, Dixon, and DWI with the construction of maps of the calculated diffusion coefficient. These data were used as material for the control group. The material of the main group was expanded by adding a single-pixel MRC, the data collection area of 2x2x2 cm was located on the most distinct pathological tissue or zone of inflammatory changes identified in the standard study, then during post-processing in the Tarquin software package, raw data was decoded as spectra with signal suppression from water, and concentration values for lactate and lip-13a were isolated. Further, native data without spectrograms and extended data sets with graphs and quantitative evaluation of the selected frequencies in a.u. were independently analyzed. False-negative, false-positive, true-negative and true-positive results of MRI and MRI+MRC were studied by the criterion of the presence or absence of tumor tissue. Malignant processes were morphologically verified by biopsy under ultrasonographic control, pancreatitis was confirmed both morphologically and dynamically by ultrasound and MRI after 6-8 weeks. Diagnostic value indicators were calculated using standard formulas, hypotheses were tested using the Fischer test, and data sets were evaluated independently by a consensus of 2 radiologists [28].

Research Results

Based on the experience of analyzing metabolites and studying trends in international spectroscopic studies, the MRI department developed a diagnostic model for pancreatic cancer, which is characterized by the presence of hyper intensive tissue in the DWI with local deformation of the typical lobular structure, obstruction of the ductal system, alternating areas of tumor tissue with restriction of ADC diffusion of 0.001-0.0016 mm^2/s and areas of predominant fibrosis [29-31]. The tumor tissue contains less fat in comparison with the parenchyma of the gland according to measurements in the dual-echo by the Dixon method, the proportion of lipids is 1-3%. According to the lactate content in spectroscopic measurements, the tumor tissue corresponds to the values of the Lactate peak of more than 1 a. u. In the presence of these signs, it was assumed that there was a tumor process in the pancreas. The data obtained in the study of the patient were compared with the data obtained on the basis of previously accumulated experience (Table 1).

In the course of work on the spectra of pancreatic tissue in various conditions, the lipid complexes of Lip 13a peaks were estimated at 1.25-1.28 ppm. In adenocarcinoma, the average value of this peak reaches 6.9 a. g, in pancreatitis-4.4 a. g., in the normal gland-1.4 a. g. The results of the study of the diagnostic value of the method are shown in Table 2. The overall accuracy of the method using MRS, calculated by the indicator of the presence of tumor tissue, reaches 95%, which is due to one case of false-negative diagnostic conclusions, but significantly exceeds the accuracy of conclusions without the use of spectroscopic criteria, where six cases of inaccurate conclusions were revealed-both in the group of patients with pancreatitis and in the group with verified pancreatic adenocarcinomas. This is confirmed by the Fisher test at a significance level of p=0.005 [32]. OR=6.88 (0.79 to 60.06). F=0.108400 ξ2=3.91 (Table 2).

Table 1: *Mean values of metabolites for various pancreatic conditions obtained in the MRI department.*

Pathology	Diffusion: SD/ADC, mm^2/s	Proportion of lipids according to the Dixon method, %	Lactate a.u.
Pancreatic cancer	0,0002/0,0013	1,79	1,7
Normal tissue	0,00035/0,0015	11,22	0
Chronic pancreatitis	0,0004/0,0018	16,47	0,1

Table 2: *Indicators of the diagnostic significance of the method of diagnosing pancreatic cancer.*

Indicator of the diagnostic method	Diagnosis of pancreatic cancer		
	taking into account the MRS data	without taking into account the MRS data (standard protocol)	3Tl MRS (literature data)
Overall accuracy	97,5% (39/40)	85% (34/40)	77%
Sensitivity	95% (19/20)	85% (17/20)	55%
Specificity	100% (20/20)	85% (17/20)	86%

For comparison, the method of MRI on a scanner with field induction of 3 T (1H-MRS) was also used according to the publication using peaks from cholesterol and fatty acid metabolites. The sensitivity of the method, according to the authors of this study, was 55%, specificity-86%, accuracy-77%, which is obviously inferior to the results of the method that combines chemical shift data and spectroscopy. For tomography with a field induction of 1.5 T scanners, such data were not found in the publications, which indicates the novelty of the proposed approach and the insufficiency of using spectroscopy on an ultra-high-field MR-scanner as a separate isolated method. The method demonstrates high accuracy in the assessment of the tumor, surpassing both the method of isolated MRC and the standard native scanning protocol [33].

Clinical Cases

Patient L. In August 2019, during an examination at the Central State Hospital of Rostov-on-Don, a tumor of the pancreatic body was detected, a histological analysis was not taken, and she independently turned to the National Research Center of Oncology for examination. MRI of the abdominal cavity from 13.08.2019, conclusion: MR-picture of the tumor process of the body and tail of the pancreas with the involvement of parapancreatic fiber, major vessels. MR-pattern of metastasis to the portal lymph node and to the retroperitoneal lymph nodes. Pancreatic hypertension. In Lac 1.015 a.u. spectroscopy, the proportion of lipids according to the Dixon method is 1.79%. Morphologically confirmed: ductal adenocarcinoma G1 in the biopsy (Figure 5).

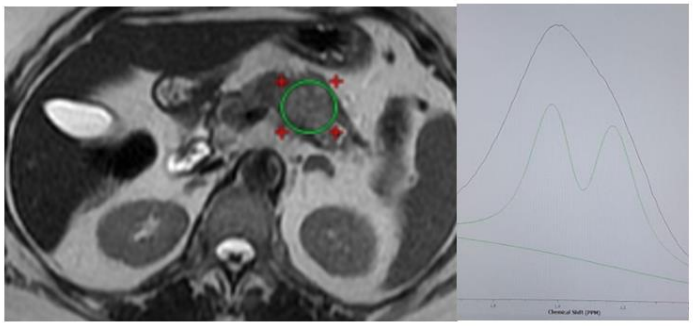

A B

Figure 5: *MRI of the pancreas: A-T2-VI with a marked tumor; B - a fragment of the spectrum with the presence of a peak of the lactate-lipid complex from the Tarquin program.*

Patient D. applied to the National Research Center of Oncology in 2019. At the time of treatment, he was ill for 1 month with negative dynamics, an MRI OBP revealed a tumor of the tail of the pancreas, and was sent to the RNIOI (NMIC of Oncology) for examination. In the tail of the pancreas, edema, ADC 0.0016-0.0019 m2 / s, the length of edematous and inflammatory changes is not less than 49x26 mm. The Virsung duct in the tail of the pancreas is locally expanded to 8 mm over 14 mm, pseudotumor pancreatitis. The proportion of lipids according to the Dixon method is 15.4%. There are no signs of a pancreatic tumor on Lac 0.0000 a.u. spectroscopy. Currently, he is diagnosed with "chronic pancreatitis" (Figure 6).

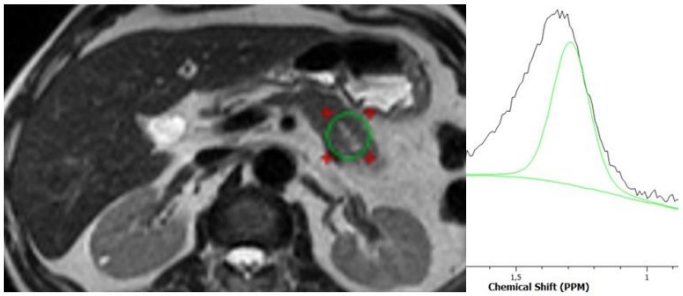

A B

Figure 6: *MRI of the pancreas: a-T2-weighted image, the general view of the pancreatitis site is outlined with a marker; b - a fragment of the spectrum with the presence of a peak of the lactate-lipid complex from the Tarquin program.*

Conclusions

MR spectroscopy can potentially be used to assess metabolic function in vivo, especially with respect to the quantification of fat, lactate, choline, citrate in the liver, pancreas, and prostate. The method can also provide useful information about other aspects of diffuse parenchymal organ disease (inflammation, dystrophy and fibrosis), help in the detection of a tumor, non-invasive assumption of its histological type, taking into account sensitivity to necrosis, can help to control the response to therapy. To demonstrate maximum diagnostic effectiveness, the MRC method should be integrated into a holistic model of multiparametric imaging, and its results should be correlated with native MRI data.

Conflicts of Interest

The authors declare no conflicts of interest.

References

1. Moon RB, Richards JH. Determination of intracellular pH by 31P magnetic resonance. J Biol Chem. 1973; 248: 7276-7278.
2. Hoult D, Busby S, Gadian D, Radda GK, Richards RE, Seeley PJ, et al. Observation of tissue metabolites using 31P nuclear magnetic resonance. Nature. 1974; 252: 285-287.
3. Bottomley PA, Edelstein WA, Foster TH, Adams WA. In vivo solvent suppressed localized hydrogen nuclear

magnetic resonance spectroscopy: a window to metabolism. Proc Natl Acad Sci. 1985; 82: 2148-2152.
4. Billewicz B, Pres GS, Majchrzak H, Zarudzki L. Differentiation between brain tumor recurrence and radiation injury using perfusion, diffusion-weighted imaging and MR-spectroscopy. Folia Neuropathol. 2010; 48: 1-92.
5. Sundgren PC. MR spectroscopy in radiation injury. Am J Neuroradiol. 2009; 30: 1469-1476.
6. Zeng QS, Li CF, Zhang K. Multivoxel 3D proton MR spectroscopy in the distinction of recurrent glioma from radiation injury. J Neurooncol. 2007; 84: 63-69.
7. Alfarouk KO, Verduzco D, Rauch C, Muddathir AK, Adil HH, Elhassan GO, et al. Glycolysis, tumor metabolism, cancer growth and dissemination. A new pH-based etiopathogenic perspective and therapeutic approach to an old cancer question. Oncoscience. 2014; 1: 777-802.
8. Ristow M. Oxidative metabolism in cancer growth. Curr Opin Clin Nutr Metab Care. 2006; 9: 339-345.
9. Estrella V. Acidity generated by the tumor microenvironment drives local invasion. Cancer res. 2013; 73: 1524-1535.
10. Colegio OR, Chu Q, Szabo AL, Chu T, Rhebergen AM, Jairam V, et al. Functional polarization of tumour-associated macrophages by tumour-derived lactic acid. Nature. 2014; 513: 559-563.
11. Ying H, Kimmelman AC, Lyssiotis CA, Chin L, Cantley LC, Depinho RA, et al. Oncogenic Kras maintains pancreatic tumors through regulation of anabolic glucose metabolism. Cell. 2012; 149: 656-670.
12. Mader I, Rauer S, Gall P, Klose U. 1H MR spectroscopy of inflammation, infection and ischemia of the brain. Eur J Radiol. 2008; 67: 250-257.
13. Amna Y, Asla P, Kimmo J, Pekka P, Olli G, Riikka I, et al. MRS reveals chronic inflammation in T2w MRI-Negative perilesional cortex – A 6-Months multimodal imaging follow-up study. Frontiers Neurosci. 2019; 73.
14. Rock JP, Scarpace L, Hearshen D. Associations among magnetic resonance spectroscopy, apparent diffusion coefficients, and image guided histopathology with special attention to radiation necrosis. Neurosurgery. 2004; 54: 1111-1119.
15. Rock JP, Hearshen D, Scarpace L, Croteau D, Gutierrez J, Fisher JL, et al. Correlations between magnetic resonance spectroscopy and image-guided histopathology, with special attention to radiation necrosis. Neurosurgery. 2002; 51: 912-919.
16. Caivano R, Lotumolo A, Rabasco P, Zandolino A, DAntuono F, Villonio A, et al. 3 Tesla magnetic resonance spectroscopy: cerebral gliomas vs. metastatic brain tumors. Our experience and review of the literature. Int J Neurosci. 2013; 123: 537-543.
17. Dezortova M. Etiology and functional status of liver cirrhosis by 31P MR spectroscopy. World J Gastroenterol. 2005; 28: 6926-6931.
18. Lim AKP, Cane D, Patel N. The relationship of in vivo 31P MR spectroscopy to histology in chronic hepatitis C. Hepatol. 2003; 37: 788-794.
19. Menon DK. Effect of functional grade and ethiology on in vivo hepatic phosphorus-31 magnetic resonance spectroscopy in cirrhosis. Hepatol. 1995; 21: 417-427.
20. Menon DK. In vivo hepatic 31P magnetic resonance spectroscopy in chronic alcoholic abusters. Gastroenterol. 1995; 108: 776-788.
21. Noren B. Separation of advanced from mild fibrosis in diffuse liver disease using 31P magnetic resonance spectro scopy. Eur J Radiol. 2008; 66: 313-320.
22. Wu B. The relationship between 31P magnetic resonance spectroscopy and the histopathology of livers of chronic viral hepatitis patients. Zhonghua Gan Zang Bing Za Zhi. 2007; 15: 338-341.
23. Li CW, Kuo YC, Chen CY, Kuo YT, Chiu YY, She FO, et al. Quantification of choline compounds in human hepatic tumors by proton MR spectroscopy at 3T. Magn Reson Med. 2005; 53: 770-776.
24. Wu B, Peng WJ, Wang PJ, Gu YJ, Li WT, Zhou LP, et al. In vivo 1H magnetic resonance spectroscopy in evaluation of hepatocellular carcinoma and its early response to transcatheter arterial chemoembolization. Chin Med Sci J. 2006; 21: 258-264.
25. MJ Roberts, HJ Schirra, MF Lavin, Gardiner RA. Metabolomics: a novel approach to early and noninvasive prostate cancer detection. Korean J Urol. 2011; 52: 79-89.
26. Lucarelli G, Rutigliano M, Galleggiante V, Giglio A, Palazzo S, Ferro M, et al. Metabolomic profiling for the identification of novel diagnostic markers in prostate cancer. Expert Rev Mol Diagn. 2015; 15: 1211-1224.
27. Varma S, Bird R, Eskin M, Dolenko B, Raju J, Bezabeh T, et al. Detection of inflammatory bowel disease by proton magnetic resonance spectroscopy (1H MRS) using an animal model. J Inflamm. 2007; 26: 4-24.
28. Album A, Norrel C. Introduction to modern epidemiology. Dat anti-cancer. 1996; 122.
29. Battini S, Faitot F, Imperiale A. Metabolomics approaches in pancreatic adenocarcinoma: tumor metabolism profiling predicts clinical outcome of patients. BMC Med. 2017.
30. Fong ZV, Winter JM. Biomarkers in pancreatic cancer: diagnostic, prognostic, and predictive. Cancer J. 2012; 18: 530-538.

31. Villanueva MH, Gironella M, Castells A, Bujanda L. Molecular markers in pancreatic cancer diagnosis. Clin Chim Acta. 2013; 418: 22-29.
32. Mehta CR, Patel NR. Exact inference in categorical data. Biometrics. 1997; 53: 112-117.
33. Tianhao SHEN, Erhu JIN. Clinical application of 3.0T proton MR spectroscopy in evaluation of pancreatic diseases. SU J Clin Radiol. 2012.